ZIBELINE INTERNATIONAL™ PUBLISHING

Water Conservation & Management (WCM)

DOI: http://doi.org/10.26480/wcm.04.2025.625.632

ISSN: 2523-5664 (Print)
ISSN: 2523-5672 (Online)
CODEN: WCMABD

RESEARCH ARTICLE

GROUNDWATER CONTROL AS A CRITICAL FACTOR IN COAL MINE SLOPE STABILITY: INTEGRATION OF SLOPE STABILITY RADAR AND BISHOP SIMPLIFIED METHOD

Harizona Aulia Rahman[a], Rusli HAR[a]*, Heri Prabowo[b], Ichsan Invanni Baharuddin[a], Ayu Nadila Rose Delfiza[b], Wahyu Riang Adeko[b]

[a]Geological Engineering, Faculty of Engineering Universitas Negeri Padang.
[b]Mining Engineering, Faculty of Engineering Universitas Negeri Padang.
**Corresponding Author Email: ruslihar@ft.unp.ac.id*

This is an open access journal distributed under the Creative Commons Attribution License CC BY 4.0, which permits unrestricted use, distribution, and reproduction in any medium, provided the original work is properly cited

Article History:

Received 11 June 2025
Revised 21 July 2025
Accepted 17 August 2025
Available online 29 September 2025

ABSTRACT

This study investigates how groundwater table (GWT) fluctuations control real-time slope deformation in an open-pit coal mine and quantifies their effect on slope safety factor (SF). The research purpose is to establish the statistical link between GWT rise and deformation velocity measured by Slope Stability Radar (SSR), estimate landslide time using the inverse-velocity method, and evaluate SF sensitivity to GWT using the Bishop Simplified Method to inform an adaptive Triggered Action Response Plan (TARP). Field monitoring with SSR was carried out over 5 days (30 Sep–4 Oct 2024) on the southern slope of Pit Banko (Tanjung Enim, South Sumatra), complemented by laboratory shear tests and stability simulations. We find a strong correlation between GWT rise (~70→90 m asl) and velocity acceleration (2.88→22.51 mm/h), culminating in a medium-scale failure. The best failure-time prediction (VCP-60) differed by only 44 minutes from the actual event. Each 5 m increase in GWT reduced SF by 18.7%, underscoring groundwater control as a critical mitigation lever. The SSR+GWT-based TARP reduced false alarms and sharpened response triggers, aligned with Indonesian regulations and international guidance. The novelty of this study is integration of real-time SSR deformation with groundwater-sensitive SF to drive threshold-based TARP decisions in a tropical open-pit context.

KEYWORDS

Slope Stability Radar (SSR), Bishop Simplified Method, Slope Safety, TARP Protocol, Groundwater Table Fluctuation, Landslide Mitigation, Open Pit Mines.

1. INTRODUCTION

Slope stability in open-pit mining is a critical aspect of geotechnical risk management, as it directly affects worker safety, equipment protection, and the overall continuity of mining operations. Slope failure can lead to workplace accidents, infrastructure damage, and significant economic losses (Le Roux et al., 2025). One of the primary factors influencing slope stability is the fluctuation of the groundwater table, which can substantially reduce the shear strength of soil or rock and thereby increase the potential for deformation and eventual landslides (Fredlund and Rahardjo, 1993; Zhang et al., 2020; Zhang and Zhang, 2021). A study using multi-physics numerical modeling, also demonstrated that water infiltration and changes in pore water pressure can drastically accelerate slope degradation, especially in formations with moderate to high permeability by (Chen et al., 2024). Similar findings were reported who independently confirmed the dominant role of groundwater table fluctuations and seepage processes in reducing the safety factor of both soil slopes and fractured rock masses (Liu et al., 2024; Beyabanaki, 2022).

The Indonesian reported that 68% of landslide incidents in coal mining operations in Indonesia were triggered by significant fluctuations in the groundwater table (Ministry of Energy and Mineral Resources, 2023). This finding is consistent with the effective stress theory proposed which states that an increase in pore water pressure due to rising groundwater tables reduces the effective stress of the soil and directly lowers the slope's Safety Factor (SF) by (Terzaghi, 1943). Recent numerical studies have even demonstrated an exponential relationship between groundwater table variations and SF reduction (Zhang et al., 2020). A real-world example of this phenomenon occurred at Pit Banko in Tanjung Enim on October 2, 2024, when high pore pressure caused by accumulated water and operational vibrations triggered a medium-scale landslide. A field-scale study on steep slopes also revealed that the amplitude and duration of groundwater table by (Frontiers Editorial, 2025)

fluctuations significantly influence head-rise velocity and pore pressure within the slope mass. As highlighted in the study of using probabilistic modelling based on rainfall data in open-pit mining areas, found that rainwater infiltration plays a major role in increasing pore pressure, which directly reduces slope stability and initiates ground failure (Shahabi et al., 2025). A previous study on landslides along the Banjir Kanal in Semarang also indicated that elevated pore pressure due to hydrogeological conditions and rock weathering was a primary factor in slope instability by (Ansosry et al., 2019). Mitigation using grouting methods proved effective in increasing soil cohesion and improving overall stability. These findings suggest that the influence of groundwater is systemic and can be effectively managed through technical interventions tailored to site-specific geomechanical conditions.

In the past decade, slope deformation monitoring technology based on Slope Stability Radar (SSR) has been widely adopted as a highly accurate early warning tool (Carlà et al., 2017; Tannant and Yan, 2020). However,

Quick Response Code	Access this article online	
	Website: www.watconman.org	**DOI:** 10.26480/wcm.04.2025.625.632

Cite The Article: Harizona Aulia Rahman, Rusli HAR, Heri Prabowo, Ichsan Invanni Baharuddin, Ayu Nadila Rose Delfiza, Wahyu Riang Adeko (2025). Groundwater Control As A Critical Factor In Coal Mine Slope Stability: Integration Of Slope Stability Radar And Bishop Simplified Method . Water Conservation & Management, 9(4): 625-632.

the real-time integration of deformation data from SSR with hydrogeological parameters-particularly the groundwater table has rarely been implemented in a comprehensive manner. Studies indicate that many early warning systems have yet to adequately incorporate hydrogeological parameters, thereby increasing the likelihood of false alarms or delayed mitigation responses to actual landslide threats (Intrieri et al., 2013; Zhang et al., 2020). Such integrative approaches are now being developed through the LEWS living-lab system, which combines real-time slope deformation and pore pressure data using a multi-sensor framework by (Carlà et al., 2024).

The effectiveness of early warning systems strongly depends on the existence of a Triggered Action Response Plan (TARP) capable of responding to varying risk levels based on deformation thresholds derived from both historical data and real-time monitoring (Intrieri et al., 2013; Carlà et al., 2017). Integrating hydrogeological parameters such as the groundwater table into TARP systems has been shown to enhance reliability. In a study demonstrated that groundwater fluctuations have an exponential impact on the reduction of the Safety Factor (SF), while emphasized that TARP systems equipped with real-time radar monitoring and hydrogeological sensors can significantly reduce false alarms and accelerate mitigation responses in high-risk areas (Tannant and Yan, 2020). From a broader perspective, highlighted the importance of using pore pressure data and probabilistic approaches in slope stability assessments, with seepage modeling serving as a key element for identifying failure risks that may go undetected under conventional deterministic methods (Radchuk et al., 2024). A similar insight was provided, who developed radar- and rainfall-based warning thresholds for the LEWS system—an approach highly relevant for application in groundwater fluctuation contexts (Li et al., 2025).

In addition, developed a failure time prediction method using the inverse velocity approach based on SSR data and deformation percentage, which serves as the statistical foundation for TARP systems (Dick et al., 2015). In a Study highlighted advancements in pore pressure monitoring technologies through IoT sensors and artificial intelligence (AI), opening significant opportunities for the development of real-time adaptive TARP systems integrating SSR and groundwater data (Alam et al. (2024). A similar AI-based prediction model was proposed by which demonstrated the effectiveness of predicting post-rainfall changes in cohesion and internal friction angle on open-pit mine slopes, using hydrological and surface deformation data as key inputs (Huang et al., 2025).

Despite these advances, no study to date has simultaneously monitored real-time slope deformation and groundwater fluctuations in an operational mine to create an adaptive warning system. This research addresses that gap by integrating a real-time SSR deformation monitoring with groundwater table analysis in open-pit coal mine to enhance landslide prediction capabilities. The correlation between groundwater fluctuations and slope deformation and stability is evaluated using Bishop's method. Additionally, an adaptive Trigger Action Response Plan (TARP) protocol is developed. This approach aims to address the limitations of existing early warning systems by incorporating hydrogeological parameters into slope stability management.

Unlike most early-warning deployments that treat deformation thresholds independently of hydrogeology, this study operationally couples real-time SSR signals with groundwater-sensitive SF changes from Bishop analysis to drive TARP triggers. The contribution is a closed-loop framework that links GWT dynamics, deformation acceleration, SF loss, and actionable thresholds. Specifically, this study aims to quantify the relationship between GWT elevation and SSR-measured deformation velocity, assess the accuracy of failure-time prediction using the inverse-velocity approach (VCP-60/180/360), evaluate SF sensitivity to GWT scenarios via Bishop, and design an adaptive TARP that integrates SSR and GWT thresholds for risk mitigation on active mining slopes.

2. MATERIAL AND METHODS

2.1 Research Location

The research was conducted on the southern slope of Pit Banko, Banko Tengah, Tanjung Enim, Muara Enim Regency, South Sumatra, Indonesia. SSR monitoring took place over 5 days 30 September – 4 October 2024. Laboratory testing and stability simulations were performed at the Geotechnical Laboratory, Department of Geological Engineering, Universitas Negeri Padang (Padang, Indonesia) in October 2024.

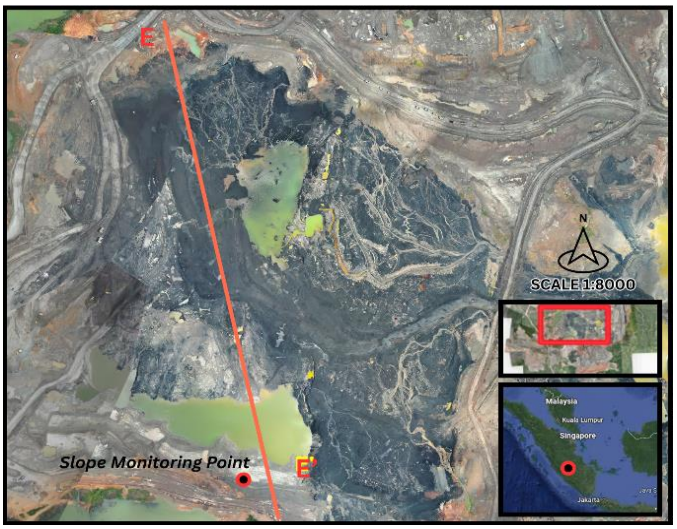

Figure 1: Map of Research and Monitoring Location

2.2 Slope Deformation Movement Pattern

Slope deformation was monitored using a Slope Stability Radar (SSR) system with GroundProbe SSR-Viewer version 8.1, which offers a measurement accuracy of up to ±0.1 mm. The monitoring was carried out over a 10-day period between January and April 2024. The primary parameters measured included deformation velocity, cumulative deformation, and inverse velocity. The deformation data were then processed by plotting deformation over time. These graphs were interpreted to identify the deformation pattern that occurred during the monitoring period leading up to the landslide event, by matching the observed trends with the deformation pattern characteristics proposed by (Broadbent and Zavodni, 1982).

a) Estimation of Failure Using Inverse Velocity Method

The test results for Combination A-0 showed an increase in pH in Landslide time prediction was conducted using velocity data from VCP 60, 180, and 360 (velocity calculation periods in minutes). These velocity values were then used to calculate the inverse velocity based on the method developed by (Fukuzono, 1985). The analysis involved identifying the intersection point between the inverse velocity forecast trendline and the x-axis (time), which served as the estimated time of the landslide occurrence.

b) Calculation of UCL and Critical Value

The slope movement velocity values were obtained from Slope Stability Radar (SSR) measurements and subsequently used to calculate the Upper Control Limit (UCL) = 3.93 mm/h and Critical Value = 9.34 mm/h following the method proposed by (Kumar and Rathee, 2017). These threshold values serve as references for identifying slope movements that exceed the primary monitoring limits. To test whether rises in GWT are associated with accelerated slope deformation and lowered SF, and whether inverse-velocity analysis can predict failure time with operational accuracy.

2.3 Bishop Simplified Stability Analysis

The results of physical and mechanical property tests provided values for unit weight (natural, dry, and saturated), cohesion, and internal friction angle for both coal and clay materials. Slope cross-section profiles, material properties, and seismic load data were subsequently used to perform the slope stability analysis. In this study, the safety factor analysis was conducted using the Bishop Simplified method developed by (Bisho, 1955).

To provide recommendations for improving slope stability in failure-prone areas, this study simulates the influence of slope geometry and groundwater table elevation on safety factor values. The simulation results are presented in tabular and graphical formats to illustrate the relationship between slope geometry, groundwater table, and the critical safety factor threshold. The slope stability analysis was performed using simulation data derived from laboratory testing of soil physical and mechanical properties, including moisture content, specific gravity, unit weight, and direct shear tests to determine cohesion (c) and internal friction angle (φ).

Groundwater table simulations were carried out under three representative scenarios: dry (65 mASL), semi-saturated (78 mASL), and fully saturated (90 mASL). These elevation levels were selected based on

initial groundwater observations and supported by literature highlighting the significant impact of groundwater fluctuations on slope stability (Zhang et al., 2020).

2.4 TARP Development

The final stage of this methodology involves integrating SSR deformation data and slope stability simulation results to develop an adaptive Triggered Action Response Plan (TARP) protocol. This protocol is based on deformation velocity thresholds calculated using statistical methods (Upper Control Limit and Critical Value) and considers the groundwater table condition as a critical parameter in mitigation decision-making. The formulation of the protocol was developed with reference to national regulations in KEPMEN No. 1827 K/30/MEM/2018 and current international guidelines, which emphasize the integration of geotechnical and hydrogeological data in the development of adaptive TARP systems (Sharon and Eberhardt, 2020; Carlà et al., 2017; The Indonesian Ministry of Energy and Mineral Resources, 2018; Sharon and Eberhardt, 2020).

3. RESULT

3.1 Deformation Behavior

Monitoring results obtained from the Slope Stability Radar (SSR) indicate a significant increase in deformation velocity on the southern slope of Pit Banko, Muara Enim Regency (Figure 2). The analysis focused on pixel P37.16, located at coordinates X = 37,000 and Y = 16,000, with a pixel size of 7.37 × 7.42 meters.

Table 1: Summary of Slope Behavior During the Five-Day Monitoring Period

Slope Behavior	Time Range	Average Velocity (mm/h)
Linier I	1 hour 57 minutes	2.88
Progressive	3 hour 34 minutes	11.521
Failure (Landslide)	21.37 local time	22.51
Linier II	2 hour 16 minutes	3.118

Table 1 shows deformation pattern detection at the study area by SSR, exhibiting a sequential deformation behavior as illustrated in Figure 3. A summary of the slope behavior during the monitoring period is presented

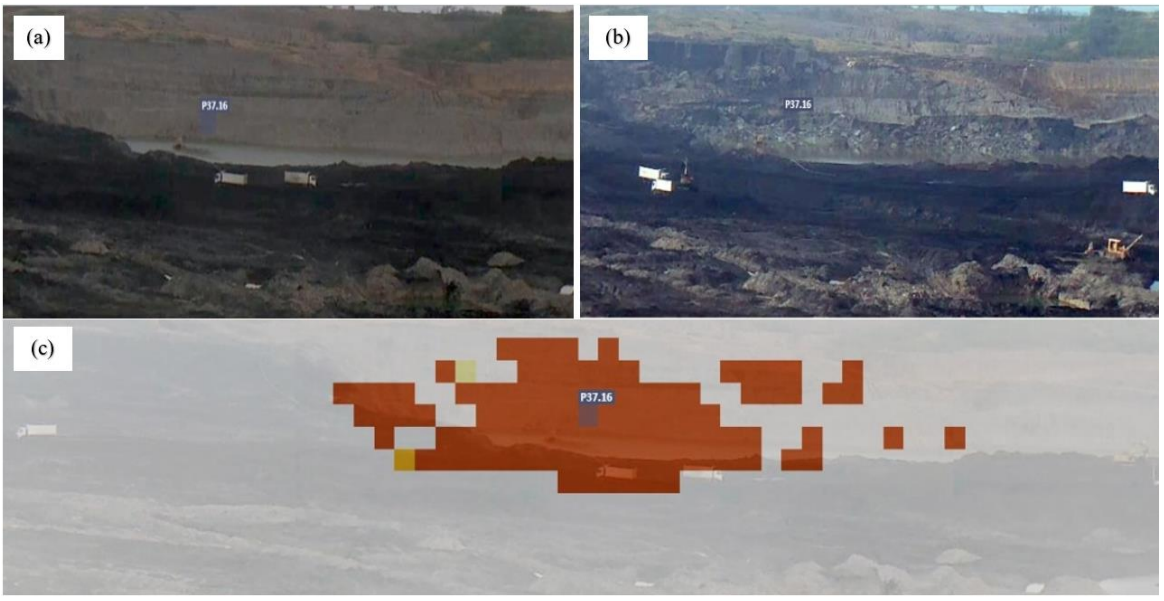

Figure 2: (a) Photograph of the slope before the landslide, (b) photograph after the landslide, and (c) monitored pixel map of the southern slope as captured by the SSR radar. The image illustrates the slope deformation behavior from September to October 2024, indicated by increasingly darker pixel coloration representing higher deformation intensity.

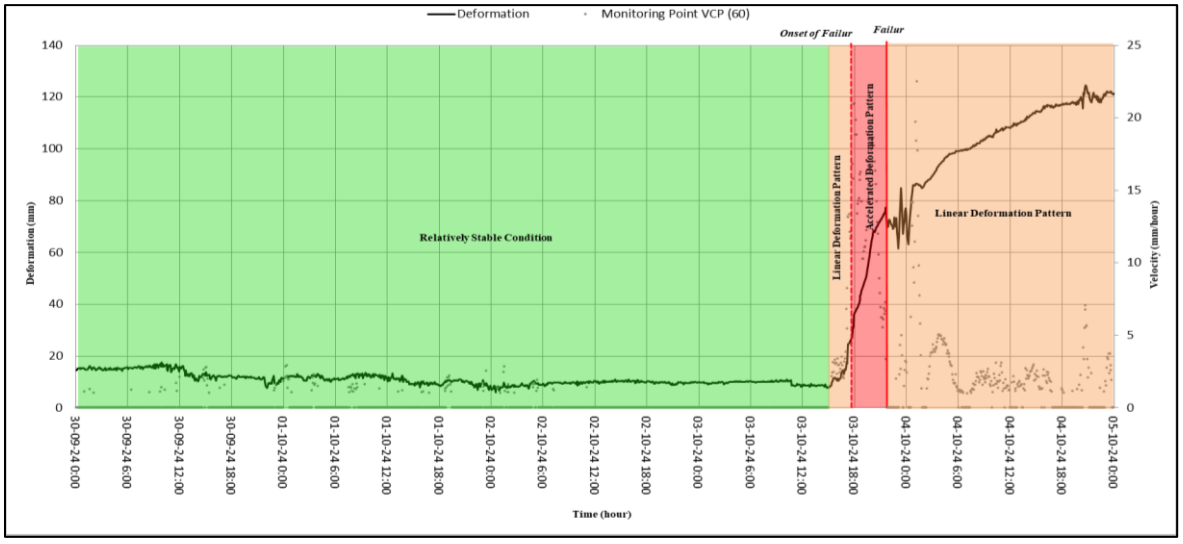

Figure 3: Deformation Graph from September 30 to October 4, 2024 in Southern Slope of Pit E

Based on the analysis of slope deformation from Figure 3 and Table 1 over a five-day monitoring period, several distinct deformation phases were identified. The initial linear deformation behavior was recorded on October 3, 2024, from 15:03 UTC to 17:00 UTC, with an average velocity of 2.88 mm/h, indicating relatively stable slope conditions after 17:03 UTC (when failure initiated), the deformation entered a progressive phase that continued until the landslide at 21:37 UTC. This phase lasted 4 hours and 34 minutes, with deformation velocity increasing from 5.4 mm/h to 20.96 mm/h, indicating a rapid acceleration toward failure.

Table 1 summarizes the slope deformation behavior as detected through SSR monitoring at Pixel P37.16. The deformation phases include an initial linear trend, a progressive acceleration, a failure event at 21:37 UTC, and a return to post-failure linear displacement. The post-failure linear behavior was recorded from 21:42 UTC on October 3 to 23:58 UTC on

October 4, with an average velocity of 3.118 mm/h, reflecting stabilization after the collapse. Average velocities for each phase clearly demonstrate an increase in deformation rate leading up to the landslide event.

3.2 Failure Time Prediction (Inverse Velocity)

The timing of the landslide was estimated using the inverse velocity method. In this approach, the predicted failure time corresponds to the intersection point of the linear forecast trendline with the x-axis, which represents time. For the VCP 60 reading, the landslide was predicted to occur on October 3 at 20:53 UTC, which is 44 minutes earlier than the actual failure time (see Figure 4). Based on the VCP 180 data, the predicted failure time was October 3, 2024, at 19:25 UTC, or 2 hours and 12 minutes earlier than the actual landslide event (Figure 5). Meanwhile, the VCP 360 reading predicted the failure at 19:20 UTC, which is 2 hours and 17 minutes ahead of the actual event (Figure 6). A summary of these estimations is presented in Table 2.

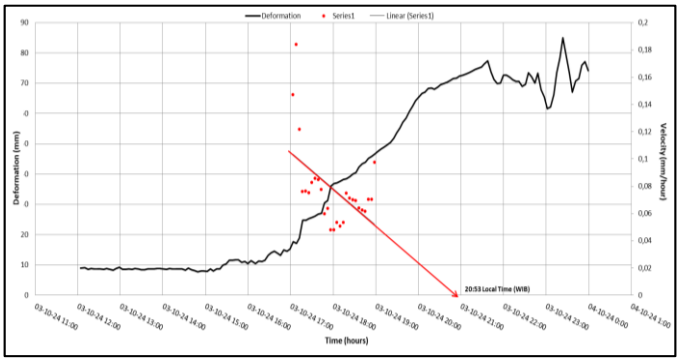

Figure 4: Landslide Time Prediction Based on VCP 60

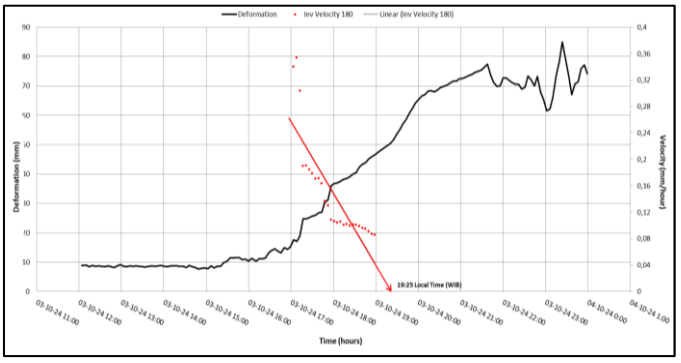

Figure 5: Landslide Time Prediction Based on VCP 180

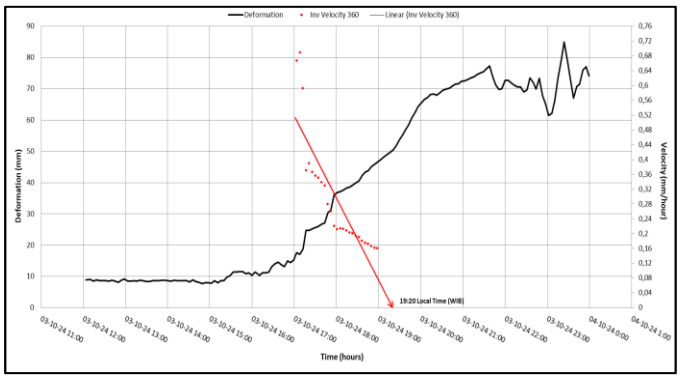

Figure 6: Landslide Time Prediction Based on VCP 360

Table 2 shows present a comparison between the predicted and actual landslide occurrence times derived from different Velocity Calculation Period (VCP) intervals using the inverse velocity method. The prediction using VCP 60 yielded the most accurate result, forecasting the failure at 20:53 UTC, which is only 44 minutes earlier than the actual event at 21:37 UTC on October 3, 2024. Predictions using VCP 180 and VCP 360 were less accurate, forecasting the failure at 19:25 UTC and 19:20 UTC respectively, which are 2 hours 12 minutes and 2 hours 17 minutes earlier than the actual landslide. These results demonstrate that shorter VCP intervals, such as VCP 60.

3.3 UCL and Critical Value Thresholds

To establish the threshold values for slope movement monitoring, the Upper Control Limit (UCL) and critical value were determined based on the average historical velocity data associated with previous landslide events. These statistical thresholds serve as key indicators to distinguish between normal deformation behavior and potentially hazardous movement. The calculated threshold values used in this study are summarized in Table 3.

Table 3: Recommended Threshold Values

Parameter	Value (mm/h)
Upper Control Limit (UCL)	3.93
Critical Value	9.34

Table 3 presents the recommended threshold values derived from slope velocity monitoring data using the VCP 60 interval. The Upper Control Limit (UCL) is determined to be 3.93 mm/h, representing the maximum allowable slope movement velocity before the system raises a red alert. This limit is operationally significant, serving as a warning point for geotechnical engineers to take preventive action when slope behavior begins to deviate from the expected range. Meanwhile, the Critical Value (CV) of 9.34 mm/h defines the threshold at which the slope deformation becomes progressive and potentially hazardous. According to Kumar and Rathee (2017), the integration of UCL and CV in early warning systems allows for improved differentiation between routine deformation and impending failure, thereby enhancing slope risk assessment frameworks.

The application of these thresholds supports a structured response strategy, enabling timely mitigation efforts in line with real-time slope behavior. In cases where the velocity exceeds the CV, the probability of landslide occurrence increases substantially, necessitating immediate evacuation or stabilization measures.

3.4 SF–GWT Sensitivity and Back-Analysis

Based on the results of laboratory testing, the physical and mechanical properties of the slope materials were determined. The physical properties include moisture content, specific gravity, and unit weight, while the mechanical properties were obtained through direct shear tests conducted under three normal load conditions: 3 kg, 6 kg, and 9 kg. These parameters were then used to calculate the Safety Factor (SF) of the slope under actual conditions. A detailed summary of the physical and mechanical test results for each sample is presented in Table 4.

Table 4: Summary of Soil Physical and Mechanical Properties

Sample	Water Content (W %)	Specific Gravity (gr/cm³)	Shear Stress (τ) kg/cm²	Normal Stress (σ) kg/cm²	Unit Weight of Claystone (gr/cm³)		
					Natural (γ)	Dry (γd)	Saturated (γsat)
A	3.120	2.2634	0.093	2.077	2.133	2.068	2.154
B	4.910	2.2353	0.186	2.410	2.015	1.920	2.061

C	5.115	2.3008	0.279	2.743	2.125	2.021	2.143
Average					2.091	2.003	2.119
Cohesion (kN/m²)					17.16		
Friction Angle (°)					9		

To determine the cohesion (c) and internal friction angle (φ) of the soil samples, an analysis of the relationship between normal stress (σ) and shear stress (τ) was carried out based on direct shear tests under three load conditions (3 kg, 6 kg, and 9 kg). The test results were plotted on a τ–σ graph (Figure 7), The slope of the regression line represents the internal friction angle (φ), while the y-intercept indicates the cohesion (c) of the soil. Based on the graphical analysis, the cohesion value for claystone was determined to be 1.75 kg/cm² or 17.16 kN/m², and the internal friction angle was 9°. These parameters were then used as input values in the slope stability simulations using the Bishop Simplified Method in the subsequent analysis.

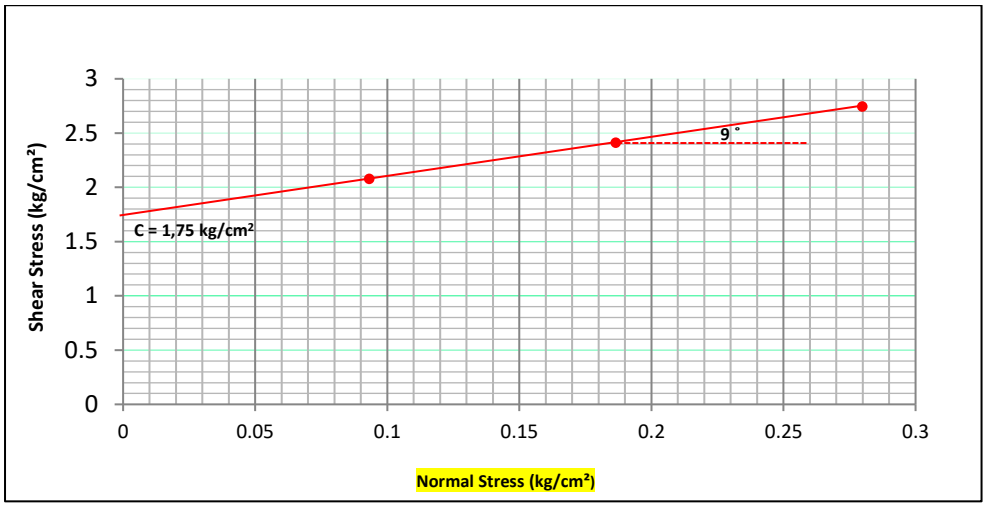

Figure 7: Shear Stress–Normal Stress Relationship for Claystone

Table 5: Back-Analysis of Groundwater Table Elevation at Time of Failure		
Groundwater Table Elevation (m asl)	**Safety Factor (SF)**	**Failure Threshold**
90 (saturated)	0,842	Unstable
85	0,943	Unstable
80	0,996	Unstable
75	1,129	Marginally Unstable
70	1,263	Stable
65 (dry)	1,342	Stable

A 10-day monitoring campaign using Slope Stability Radar (SSR) on the southern slope of coal mining in Pit Banko revealed a strong correlation between rising groundwater table (GWT) elevations and slope deformation dynamics. Due to the lack of direct rainfall and piezometric measurements at the site, the groundwater elevation at the time of failure was estimated through back-analysis simulations. These simulations involved adjusting the groundwater table elevation to determine its impact on the slope's Safety Factor (SF), where failure was assumed to occur when SF < 1.2, based on typical geotechnical stability thresholds.

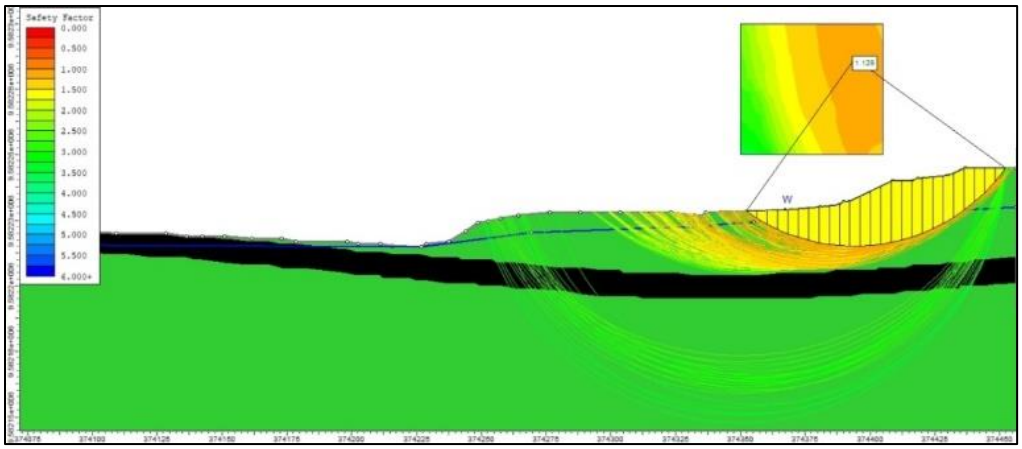

Figure 8. Slope Stability Simulation at Groundwater Elevation 75 m (SF = 1.129)

The simulation results of groundwater elevation and corresponding slope deformation behavior (Figure 8) reveal that during the early linear deformation phase-recorded at a velocity of 2.88 mm/h. The groundwater table was likely positioned at approximately 70 meters above sea level. As the groundwater table continued to rise to between 75 and 90 meters, the Safety Factor (SF) declined below the critical threshold of 1.2, triggering progressive slope movement. This phase was marked by deformation

velocities exceeding 9.34 mm/h, culminating in a peak velocity of 22.51 mm/h with an inverse velocity ≈ 0, coinciding with the occurrence of a moderate-scale landslide at 21:37 UTC.

The physical and mechanical properties of the claystone material further reinforce the slope's hydrogeotechnical vulnerability. Laboratory testing revealed water content ranging from 3.12% to 5.115%, an average saturated unit weight of 2.119 g/cm^3, cohesion of 17.16 kN/m^2, and an internal friction angle of only 9°-a combination that indicates limited shear strength under elevated pore water pressure. Groundwater simulations showed that every 5-meter increase in groundwater elevation

resulted in an average SF reduction of 18.7%, highlighting the exponential influence of groundwater on slope stability.

Groundwater table is identified as the dominant controlling factor in slope

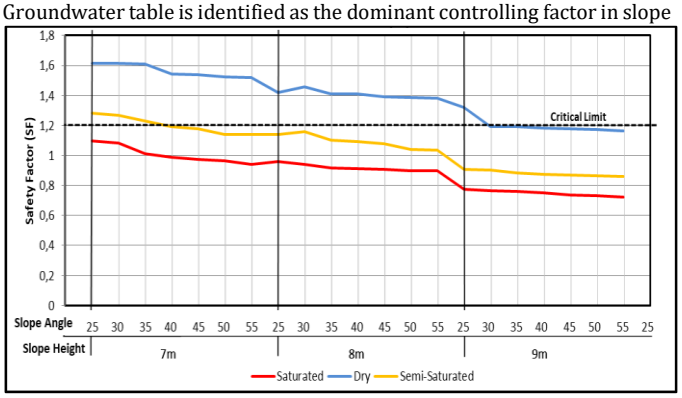

Figure 9: Graph of the Relationship Between Slope Geometry and Slope Safety Factor (SF) Under Various Groundwater Table Conditions

instability, as confirmed through three key mechanisms: (1) elevated pore water pressure during the progressive phase reduces effective stress; (2) increased moisture content leads to cohesion loss of the slope material; and (3) full saturation increases the soil's saturated unit weight, enhancing driving forces. These conditions are further aggravated by operational vibrations from heavy machinery, measured at 0.05g, which accelerate the imbalance of saturated soil mass. To address this instability, slope geometry and groundwater conditions were further simulated to recommend slope stabilization strategies. The results, illustrated in Figure 9, confirm the exponential relationship between rising groundwater table and declining SF, where slopes steeper than 45° and groundwater elevation above 80 meters yield SF values below 1.2. Figure 10 shows that introducing 0.05g vibration causes an additional 12–18% reduction in SF, significantly exacerbating failure risk under high saturation conditions.

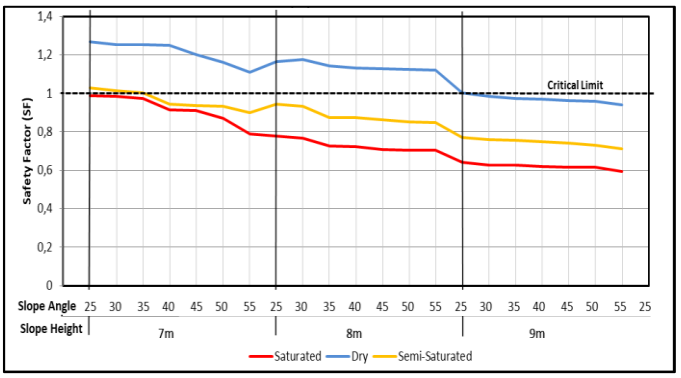

Figure 10: Graph of the Relationship Between Slope Geometry and Safety Factor (SF) Under Various Groundwater Table Conditions After the Addition of 0.05g Vibration

4. Discussion

The results of this study demonstrate a significant correlation between fluctuations in the Groundwater Table (GWT) and slope deformation behavior in Southern Slope of Pit Banko Over a 10-day monitoring period using Slope Stability Radar (SSR), the rise in GWT elevation from 70 to 90 meters above sea level (mASL) was found to accelerate slope deformation velocity from 2.88 mm/h to 22.51 mm/h. The peak deformation coincided with a moderate landslide event on October 3, 2024, at 21:37 UTC. The predicted landslide time, derived using the inverse velocity method, deviated by only 44 minutes from the actual event, underscoring the predictive accuracy achieved through the integration of SSR data and the Bishop Simplified method.

Stability analysis using the Bishop Simplified method revealed that each 5-meter increase in MAT elevation resulted in an average 18.7% reduction in the Safety Factor (SF). The actual SF values at the time of failure were consistently below the critical threshold of 1.2, reinforcing the critical role of GWT in slope stability. This finding aligns with the results of previous studies which emphasize groundwater as a dominant factor in slope failure mechanisms by (Zhang et al., 2020; Liu et al., 2024; Chen et al., 2024).

The hydrogeotechnical vulnerability of the slope is further confirmed by the physical and mechanical properties of the claystone material. The moisture content ranged between 3.12% and 5.12%, with a saturated unit weight of 2.12 g/cm^3, cohesion of 17.16 kN/m^2, and an internal friction angle of only 9°. These characteristics indicate a limited capacity to withstand pore pressure under saturated conditions. The GWT simulation results reveal that full saturation not only increases the driving force due to higher unit weight, but also reduces effective stress and shear strength-ultimately accelerating slope failure.

The dominant role of groundwater in triggering slope instability is evident through three primary mechanisms: (1) increased pore water pressure reduces effective stress; (2) increased moisture content lowers material cohesion; and (3) full saturation raises the saturated unit weight, thereby increasing the driving force. These effects were exacerbated by operational vibrations from heavy equipment, estimated at 0.05g, which further destabilized the saturated slope mass.

To mitigate these risks, simulations were conducted to evaluate the effect of lowering the GWT through vertical drainage systems installed 25 meters below the slip surface. The results showed a SF increase from 1.014 to 1.538 (a 65.9% improvement) under static conditions, and from 0.972 to 1.252 (a 77.6% improvement) under dynamic conditions. This intervention also resulted in a 32% reduction in deformation velocity, highlighting its effectiveness in improving slope stability. As a strategic response, a Triggered Action Response Plan (TARP) was developed to integrate hydrogeological and geotechnical parameters in an adaptive risk management framework as shown in Table 6.

Table 6: Adaptive Protocol of TARP

Trigger Level	Trigger Condition	Action	Description
Stable (TARP 1-2)	-	-	1. Monitoring team continuously checks data parameters and deformation trends 2. Regular monitoring of the groundwater table
Linear Deformation (TARP 3)	Groundwater Table > 75 mASL Velocity > 3.94 mm/h *No acceleration observed*	Email notification to Geotech team	1. Inform location, rate, and extent of slope movement. 2. Check for changes in deformation pattern. 3. Activate dewatering pumps (field team).
Progressive Deformation (TARP 4)	Groundwater Table > 80 mASL Velocity > 9.34 mm/h *Acceleration observed*	Phone call and email to Geotech team	1. Provide critical area information. 2. Conduct deformation velocity analysis.

			3. Predict potential failure time based on inverse velocity method. 4. Execute field evacuation procedures.

To enhance operational safety and slope failure response strategies, an adaptive Triggered Action Response Plan (TARP) was developed, integrating real-time deformation and groundwater table data. This TARP is structured into three escalation levels-Stable (TARP 1–2), Linear Deformation (TARP 3), and Progressive Deformation (TARP 4) - based on key threshold parameters including deformation velocity and groundwater table elevation. These thresholds were calibrated using SSR monitoring data and statistically derived values such as the Upper Control Limit (UCL) and Critical Value (3.94 mm/h and 9.34 mm/h, respectively), based on historical slope failure trends. The framework is aligned with the Guidelines for Open Pit Slope Design Series and national regulations from which emphasize the integration of geotechnical and hydrogeological parameters in real-time early warning systems (Sharon and Eberhardt, 2020; Carlà et al., 2017; the Indonesian Ministry of Energy and Mineral Resources, 2018). The adaptive SSR-Groundwater Table based TARP protocol developed in this study has proven effective in enhancing monitoring reliability, minimizing false alarms, and accelerating mitigation responses in high-risk slope areas.

5. Conclusion

Real time integration of SSR deformation with groundwater-sensitive Bishop analysis shows that GWT rise is the dominant driver of acceleration and failure on the studied mine slope. Across 5 days of monitoring, velocity increased from 2.88 to 22.51 mm/h as GWT rose from ~70 to 90 m asl; inverse-velocity analysis (VCP-60) predicted failure within 44 minutes of the actual time. SF decreased by ~18.7% for every 5 m GWT rise, crossing the operational threshold (SF < 1.2) under higher saturation. An SSR+GWT-based TARP with UCL 3.93 mm/h and CV 9.34 mm/h delivered actionable, low-false-alarm triggers aligned with national and international guidance. Groundwater control is the most effective lever to suppress acceleration and recover SF, implementing targeted dewatering and drains should be prioritized in scheduling and budgeting for slope risk reduction.

Author Contributions

Harizona Aulia Rahman: Conceptualization, Research methodology, Data curation, Data analysis, Project administration; Rusli HAR: Corresponding Author, writing research drafts, editing, finalizing articles; Heri Prabowo: Grammar and scientific writing; Ichsan Invanni Baharuddin: Supervision, Grammar and Scientific writing Ayu Nadila Rose Delfiza: Surveyor, collecting research data, designing research equipment, testing; Wahyu Riang Adeko: writing the research draft

Acknowledgement

The authors would like to thank: All members involved in this research, Department of Geological Engineering and Mining Engineering, Faculty of Engineering, Universitas Negeri Padang, and Coal Mining in Tanjung Enim Area, Muara Enim Regency, South Sumatra, Indonesia.

References

Alam, M. J. B., Manzano, L. S., Debnath, R., and Ahmed, A. A., 2024. Monitoring slope movement and soil hydrologic behavior using IoT and AI technologies: A systematic review. Hydrology, 11(8), Pp. 111. https://doi.org/10.3390/hydrology11080111

Ansosry, A., Rahman, H. A., and Ramadhan, F., 2019. Landslide mitigation of Banjir Kanal Semarang, with grouting method. Journal of Physics: Conference Series, 1387(1), 012099. https://doi.org/10.1088/1742-6596/1387/1/012099

Beyabanaki, S., 2022. Impact of groundwater table fluctuation on stability of jointed rock slopes and landslides. GeoHazards, 2(2), 15. https://www.mdpi.com/2673-7094/2/2/15

Bishop, A. W., 1955. The Use of Slip Circle in The Stability Analysis of Slopes. Geotechnique, 5(1), 7–17. https://doi.org/10.1680/geot.1955.5.1.7

Broadbent, C. D., and Zavodni, Z. M., 1982. Influence of rock structure on stability. Stability in surface mining, 3(2).

Carlà, T., Intrieri, E., Di Traglia, F., Nolesini, T., Gigli, G., and Casagli, N., 2017. Guidelines on the use of inverse velocity method as a tool for setting alarm thresholds and forecasting landslides and structure collapses. Landslides, 14, Pp. 517–534. https://doi.org/10.1007/s10346-016-0731-5

Carlà, T., Segoni, S., and Casagli, N., 2024. Inform@Risk: A living-lab early warning system prototype for rainfall-induced landslides in urban settlements. Natural Hazards and Earth System Sciences, 24(7), Pp. 1843–1862. https://nhess.copernicus.org/articles/24/1843/2024/

Chen, W., Li, S., and Zhou, Q., 2024. Multiphysics modeling of slope degradation under water infiltration in fractured rocks. Engineering Geology, 322, 107011. https://doi.org/10.1016/j.enggeo.2024.107011

Dick, G., McKinnon, R., and Stewart, R., 2015. Slope stability radar for monitoring mine walls. The Journal of The Southern African Institute of Mining and Metallurgy, 115(7), 677–683. https://www.saimm.co.za/Journal/v115n07p677.pdf

Fredlund, D. G., and Rahardjo, H., 1993. Soil mechanics for unsaturated soils. John Wiley and Sons.

Frontiers Editorial. 2025. Groundwater recharge in a steep mountain slope and its implications. Frontiers in Earth Science, 13, 1612208. https://www.frontiersin.org/articles/10.3389/feart.2025.1612208

Fukuzono, T., 1985, A new method for predicting the failure time of a slope, Proceedings of the fourth international conference and field workshop on landslides, Tokyo: Japan Landslide Society, pp. 145–50

Huang, Y., Zhang, H., and Lin, J., 2025. AI-powered slope stability risk prediction in open-pit mines. Journal of Mining Science, 61(2), Pp. 241–256. https://doi.org/10.1007/s12345-025-01234-y

Indoneisan Ministry of Energy and Mineral Resources. 2018. Ministerial Decree No. 1827 K/30/MEM/2018 regarding Guidelines for Good Mining Practices. Ministry of Energy and Mineral Resources. Jakarta.

Indoneisan Ministry of Energy and Mineral Resources. 2023. Statistik Insiden Longsor di Tambang Batubara Indonesia. Jakarta: Direktorat Jenderal Mineral dan Batubara.

Kumar, A., and Rathee, R., 2017. Monitoring and Evaluating of Slope Stability for Setting out of Critical Limit at Slope Stability Radar. International Journal of Geo-Engineering, 8(1). https://doi.org/10.1186/s40703-017-0054-y

Intrieri, E., Gigli, G., Casagli, N., Nadim, F., and Kalsnes, B., 2013. Brief communication "Landslide early warning system: toolbox and general concepts". Natural Hazards and Earth System Sciences, 13, Pp. 85–90. https://doi.org/10.5194/nhess-13-85-2013

Le Roux, R., Sepehri, M., Khaksar, S., and Murray, I., 2025. Slope stability monitoring methods and technologies for open-pit mining: A systematic review. Mining, 5(2), 32. https://doi.org/10.3390/mining5020032

Li, P., Xu, Q., Liu, J. et al., 2025. Establishing radar-derived rainfall thresholds for a landslide early warning system: a case study in the Sichuan Basin, Southwest China. Sci Rep 15, 26308. https://doi.org/10.1038/s41598-025-10464-6

Liu, J., Feng, S., Zhang, Y., and Wang, D., 2024. Slope stability analysis method considering the rainfall hydrology process. Engineering Geology, 333, 108081. https://doi.org/10.1016/j.enggeo.2024.108081

Radchuk, R., Schlüter, M., and Kolditz, O., 2024. Probabilistic slope stability assessment integrating pore water pressure and seepage modeling. Georisk: Assessment and Management of Risk for Engineered Systems and Geohazards, 18(1), Pp. 1–15. https://doi.org/10.1080/17499518.2024.1982123

Shahabi, H., Shirzadi, A., Ahmad, B. B., Ahmad, A., Pham, B. T., Hossain, M. S., Shukor, N. A. A., and Lee, S., 2025. Rainfall-based probabilistic modeling for landslide susceptibility assessment in open-pit mines. Global Journal of Environmental Science and Management,

11(3), Pp. 875–896. https://doi.org/10.22034/GJESM.2025.03.10

Sharma, A., Kumar, S., and Patel, R., 2023. IoT-based groundwater table monitoring for sustainable mining. Water, 15(4), 671. https://doi.org/10.3390/w15040671

Sharon, R., and Eberhardt, E., 2020. Guidelines for slope performance monitoring (Guidelines for Open Pit Slope Design Series; Vol. 5). CSIRO Publishing. https://doi.org/10.1071/9781486311002

Tannant, D. D., and Yan, M., 2020. Monitoring open pit mine highwalls with radar. International Journal of Mining Science and Technology, 30(1), Pp. 17–22. https://doi.org/10.1016/j.ijmst.2019.12.001

Terzaghi, K., 1943. Theoretical soil mechanics. John Wiley & Sons.

Zhang, L., Wang, Y., and Sun, D., 2020. Analysis of slope stability under changing groundwater conditions. Geotechnical and Geological Engineering, 38, 1477–1490. https://doi.org/10.1007/s10706-020-01213-4

Zhang, W., and Zhang, Z., 2021. Evaluation of slope stability with varying groundwater tables using numerical simulation. International Journal of Geomechanics, 21(2), 04020231. https://doi.org/10.1061/(ASCE)GM.1943-5622.0001892